

Cite this article as: Li Xijie, Li Zhipeng, Liu Jianglin, et al. Effect of Heat Treatment Temperature on Microstructure and Corrosion Resistance of TA1/304 Composite Plates[J]. Rare Metal Materials and Engineering, 2026, 55(06): 1409-1418. DOI: <https://doi.org/10.12442/j.issn.1002-185X.20250133>.

ARTICLE

Effect of Heat Treatment Temperature on Microstructure and Corrosion Resistance of TA1/304 Composite Plates

Li Xijie¹, Li Zhipeng¹, Liu Jianglin^{1,2,3}, Zhao Linchao¹, Tang Yuping¹, Liang Jianguo^{1,2,3,4}

¹ College of Mechanical Engineering, Taiyuan University of Technology, Taiyuan 030024, China; ² Engineering Research Center of Advanced Metal Composites Forming Technology and Equipment, Ministry of Education, Taiyuan 030024, China; ³ State Key Laboratory of Metal Forming Technology and Heavy Equipment, Taiyuan 030024, China; ⁴ Xinjiang Institute of Intelligent Equipment, Aksu 843000, China

Abstract: The corrosion resistance and corrosion mechanism of TA1/304 composite plates after heat treatment at different temperatures were studied by simulating electrochemical experiments in artificial seawater (3.5wt% NaCl solution). The interfacial diffusion and microstructure evolution were studied. The results show that the diffusion range of interfacial elements and the thickness of the diffusion layer change with the heating temperatures. Because of its special structure and composition, the TA1/304 composite plate shows excellent corrosion resistance in Cl⁻-containing corrosive media, and its corrosion resistance is significantly better than that of ordinary steel plates. Meanwhile, it is found that the heat treatment process of the composite plate has a significant impact on its corrosion resistance. After annealing at 600 °C, the corrosion resistance of the composite plate is improved, and corrosion properties of rolled surface is much greater than that of the cross-section. This research achievement provides important theoretical basis and technical support for the further application of TA1/304 composite plates in fields with strict corrosion resistance requirements, such as chemical engineering and marine engineering.

Key words: titanium/steel composite plate; heat treatment temperature; metallographic microstructure; electrochemical corrosion; diffusion behavior

1 Introduction

Corrosion-induced material degradation causes substantial annual economic losses, particularly for marine construction steels^[1-2]. 304 stainless steel, as the most widely used stainless steel, is versatile with good heat resistance, low-temperature strength, mechanical properties, hot workability, and no heat-treatment hardening. Although it exhibits good resistance to atmospheric corrosion, it is prone to localized corrosion in Cl⁻-containing marine environments. Compared to traditional stainless steel, titanium and its alloys are increasingly adopted in marine settings due to low density, high specific strength, excellent corrosion resistance, heat resistance, non-magnetism, good biocompatibility^[3-5], and particularly superior corrosion resistance. Titanium/steel composite plates, which integrate the merits of both metals, are key corrosion-resistant structural

materials for marine engineering, rail transportation, petrochemicals, and healthcare^[6], thus becoming indispensable in modern chemical and pressure vessel industries.

However, research on hot rolling of TA1/304 composite plates remains restricted. Titanium/steel composite plates are primarily prepared via diffusion, explosion, and rolling methods. The latter dominates due to controllable processes, high efficiency, and industrial scalability^[7-9]. Notably, significant differences in physical properties and metallurgical incompatibility between titanium and steel hinder the formation of adequate hot-rolled bonding structures. During rolling, residual stresses and brittle intermetallic compounds (IMCs) form at the interface, causing microstructural inhomogeneity and interfacial degradation, ultimately reducing titanium-steel bonding strength^[10]. Our team has achieved high-bonding-strength

Received date: June 14, 2025

Foundation item: General Program of National Natural Science Foundation of China (52075359); National Key Research and Development Program (2018YFA0707300); Lvliang Science and Technology Guidance Special Key R&D Project (2022XDHZ08); Postdoctoral Science Foundation of China (2020M670710)

Corresponding author: Liu Jianglin, Ph. D., Associate Professor, College of Mechanical Engineering, Taiyuan University of Technology, Taiyuan 030024, P. R. China, E-mail: liujianglin@tyut.edu.cn

Copyright © 2026, Northwest Institute for Nonferrous Metal Research. Published by Science Press. All rights reserved.

titanium-steel composites via experimental treatments. Wang et al.^[10] prepared titanium/steel composite plates via hot rolling at 700–950 °C with 30% reduction. Bonding strength first increases and then decreases with the increase in temperature, peaking at 311 MPa at 850 °C, where the cladding is less contaminated by the base material, yielding good bonding and expanding practical applications. Thus, improving bonding strength, reducing costs, and manufacturing fine-corrosion-resistant titanium/steel composites remain research hotspots.

As a key corrosion-resistant structural material, titanium/steel composite plates expose their titanium surfaces to diverse corrosive media during service^[11]. For instance, in seawater heat exchangers, acetic acid distillation towers, and petrochemical vessels, the titanium layer of such composites is directly in contact with the corrosive environments. However, research on their corrosion behavior remains restricted, particularly regarding the effect of microstructure on the corrosion performance of pure titanium and titanium/steel composites, which remains controversial. Garbacz et al.^[12] concluded that the corrosion resistance of Ti nanocrystals in 0.9wt% NaCl solution is slightly worse than that of coarse-crystalline Ti, and the passivation film on the surface of coarse-crystalline Ti is more homogeneous compared to that of nanocrystalline Ti. Hoseini et al.^[13] showed that the corrosion behavior of pure titanium is directly related to the microstructural characteristics. However, Luo et al.^[5] found that pure titanium after iso-channel corner extrusion has smaller grain size, more grain boundaries, and increased dislocation density than pristine pure titanium specimens. In Ringer's simulated body fluid and simulated oral saliva environments, pure titanium extruded by equal channel corner extrusion has a smaller self-corrosion current density, a larger polarization resistance, a larger impedance radius, and better corrosion resistance than pristine pure titanium. The influence of microstructure on the corrosion behavior of titanium and titanium alloys has been reported in several cases. Cvijović-Alagić et al.^[14] studied the electrochemical behavior of Ti-13Nb-13Zr and Ti-6Al-4VELI alloys with martensitic microstructures and concluded that Ti-6Al-4VELI alloy with a fully martensitic microstructure has better corrosion resistance than Ti-13Nb-13Zr alloy.

Due to the excellent corrosion resistance of titanium, it is difficult for corrosive media to enter the inner steel plate. However, in the practical application of offshore engineering, the surface titanium layer is often thin, which is prone to scratch and abrasion, exposing the substrate steel, and leading to more serious corrosion. Mudali et al.^[15] pointed out that the explosion welding process significantly affects the corrosion resistance of the titanium-stainless steel composite interface, and corrosion at the bonding interface in nitric acid solution is very obvious. In the study of corrosion behavior for titanium/steel composite plates, attention should be paid to not only the corrosion-resistant titanium layer, but also the corrosion behavior of the composite interface. Liu et al.^[16] studied the corrosion behavior of TA2/A36 composite plate in the marine environment, and the results showed that there is an

accelerated corrosion effect at the composite interface, while deep accelerated corrosion cracks are observed. Lu et al.^[17] used explosion welding to connect TA1 and 304 stainless steel to obtain the composite plate, which has good corrosion resistance between different raw materials. Li et al.^[18] found that the corrosion behavior of titanium-steel composite plate is coordinated by various corrosion behavior in the near interface area and the far interface area. Under the combined action of different corrosion behavior, the corrosion rate at the interface of titanium-steel composite plate is faster than that at the far interface area. Pu et al.^[19] found that the interface hardness of hot-rolled titanium-steel composite plates is the lowest, and the shear strength is the highest at an annealing temperature of 550 °C. At the same time, the corrosion resistance of the titanium plates also shows a significant improvement, indicating that this temperature provides favorable conditions for enhancing the corrosion resistance of the plates. The presence of IMCs and the complex microstructure in the composite interface have a significant effect on the corrosion resistance of composite plate, so it is very important to study the interface structure and corrosion behavior of TA1/304 composite plate.

2 Experiment

The experimental material was hot rolled TA1/304 composite plate, which combined the excellent corrosion resistance of titanium and the mechanical properties of steel. The base material was 304 stainless steel, and the compound material was TA1. The hot rolling temperature was 850 °C, and the thickness of titanium plate and stainless steel was 2 and 3 mm, respectively. The flowchart of experimental process is shown in Fig.1.

The titanium-steel combined surface was polished with a flat grinder and an angle grinder to remove the oxidized layer and stains, which helped to increase the surface roughness and enhance the bonding strength. The TA1/304 bilayer structure was then prepared to form the billet, followed by gas tungsten arc welding with Cu70Ni30 filler wire to achieve the joining of the two components. The assembled TA1/304 composite plate was placed into an argon gas heating furnace. The heating temperature was 850 °C and the holding time was 90 min. Then, the plate was subjected to the rolling process. The upper roll was corrugated and in contact with the 304 plate, and the lower roll was a regular flat one in contact with the TA1 plate. The profile of the corrugated roll was a sinusoidal curve with an amplitude of 0.7 mm, consisting of 75 corrugations, and the diameter of the roll was 150 mm, which was the same as the diameter of the lower flat roll. The rolled composite plates (Origin) were subjected to annealing heat treatment at 550, 600, and 650 °C for 1 h.

The specimens used for characterization were polished with sandpaper and then sequentially polished with diamond polishing solution and 0.3 μm silica. After polishing, the specimens were ultrasonically cleaned in alcohol for 3 min and dried with cold air. The microstructure and morphology of the matrix and cross-section interface of the TA1/304 composite

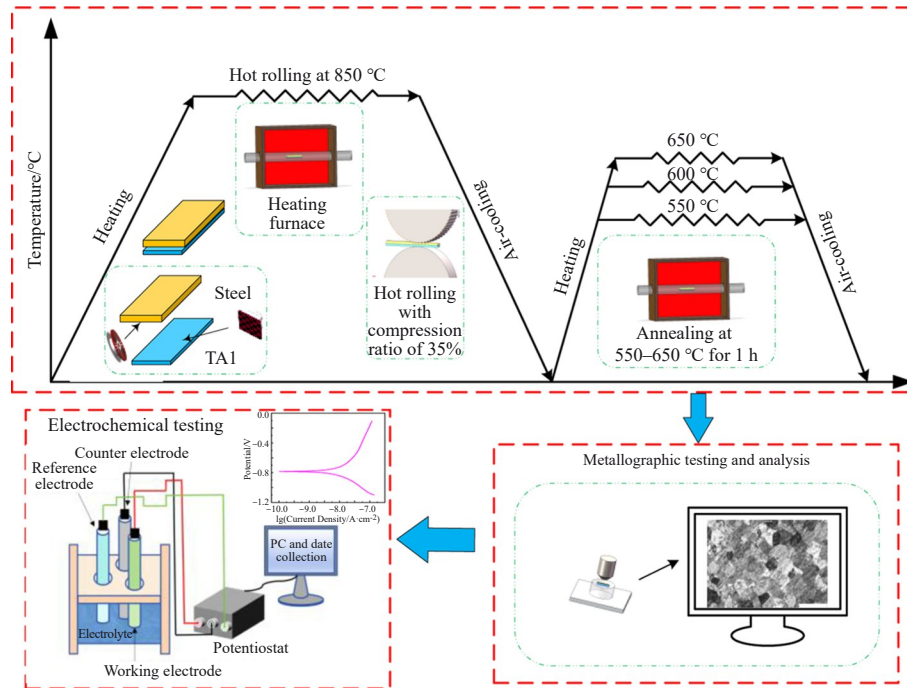


Fig.1 Flowchart of the experimental process

plates were observed by a 3D profilometer and optical microscope (OM). The elemental distribution of the specimen cross-section was analyzed by energy disperse spectroscope (EDS).

To evaluate the difference in corrosion resistance of TA1/304 composite plate, dynamic polarization curve tests and electrochemical impedance spectroscopy (EIS) tests were performed. The rough-machined specimens of the composite plates were cut, as shown in Fig.2. RD and ND mean rolling direction and normal direction, respectively. The surface layer was fixed with A/B adhesive, and the internal guide wires were relocated out. The simulation solution was a 3.5wt% NaCl solution, and all subsequent corrosion tests were performed in the same solution. Electrochemical corrosion measurements were conducted at room temperature using a CHI660D electrochemical workstation, with three parallel tests for each specimen to ensure reproducibility. A classic three-electrode system was used, with a TA1/304 composite plate as the working electrode, a platinum electrode as the auxiliary

electrode, and a saturated calomel electrode as the reference electrode. The specimens were held in a jig and immersed in NaCl solution. The open-circuit potential was measured before the test, and the alternating current (AC) impedance was tested after the potential was stabilized. The electrochemical impedance spectrum was tested at a frequency of 10^{-2} – 10^5 Hz with an amplitude of 0.01 V, and then the dynamic polarization curve was tested. The initial scanning potential was set to -1.0 V, the final potential was 0.5 V, the scanning speed was 10 mV/s, and the sensitivity was 1×10^{-4} .

3 Results and Discussion

3.1 Microstructure

Fig.3 shows original microstructure of the as-received TA1

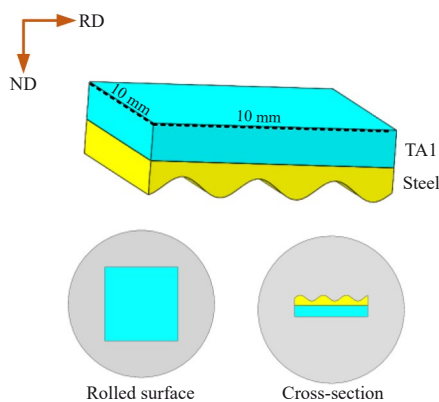


Fig.2 Schematic diagrams of specimens used for corrosion tests

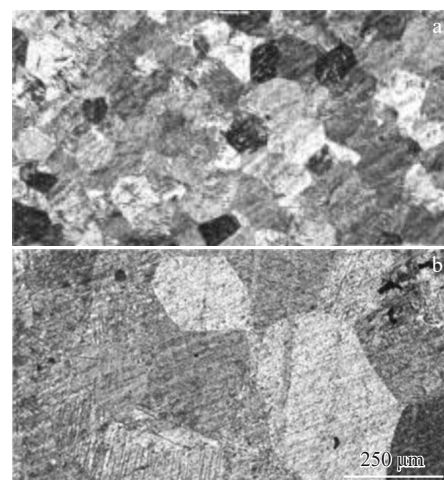


Fig.3 Microstructures of TA1 plate before rolling: (a) as-received; (b) preheated at 850 °C for 1.5 h

cladding in the TA1/304 composite plate, as well as the microstructure of TA1 after preheating at 850 °C before hot rolling. Fig. 4a shows that the grains of as-received TA1 plate before rolling are uniformly distributed and equiaxed, and the average grain size is about 70 μm . After preheating at 850 °C for 1.5 h (Fig. 3b), the average grain size is obviously increased to about 150 μm .

The microstructure morphologies of TA1/304 composite plates after different annealing heat treatments are shown in Fig. 4. Fig. 4a shows that the grains without heat treatment have great deformation and are obviously refined and elongated along RD. The equiaxed grains are violently deformed, and typical fibrous microstructures are extensively observed. Most of the original grain boundaries disappear. Fig. 4b–4c show that after annealing at 550 °C, the fibrous grains gradually disappear and are replaced by a lamellar and fine equiaxed microstructure. After annealing at 650 °C, the grain boundaries are distinct, and the grains are completely spheroidized.

Fig. 5 shows the microstructures of cross-section of the Origin and annealed TA1/304 composite plates. As shown in Fig. 5a–5b, after rolling, the microstructure near the TA1 side of the bonding interface is obviously drawn into the interfacial region. And the grain size near the interface is smaller, showing obvious fibrous deformation as a result of the high

rolling force and severe shear stress during the hot rolling process. The direction of metal flow is consistent with RD, but the flow effect gradually diminishes with the increase in temperature. This is because the higher temperature promotes grain growth and nucleation, and the microstructure is more uniform. The recrystallization occurs in the TA1 side during the heat treatment process, and fibrous grains gradually become equiaxed. With the increase in annealing temperature, the degree of grain elongation on the TA1 side decreases, and after annealing at 650 °C, the grains show an equiaxed morphology^[20]. There is an extensive austenitic microstructure on the steel side, the deformation is not obvious, and the crystal structure is relatively stable, which is probably due to the small deformation of the steel side in the hot rolling process.

3.2 Hardness

Fig. 6 shows the interfacial hardness distribution of the TA1/304 composite plate, where 0 represents the center of the interface, the left side of the interface is 304 stainless steel, and the right side is the TA1 side. The microhardness curves at the peaks and valleys of the bonding interfaces show roughly similar trends, and at the interface between the TA1 and steel sides, the hardness of the steel and TA1 decreases sharply after annealing. This is because stress can promote recrystallization nucleation and inhibit the growth of recrystallized grains, thus refining the grains and increasing the hardness,



Fig. 4 Microstructures of TA1/304 composite plates at different states: (a) Origin; (b) 550 °C; (c) 650 °C

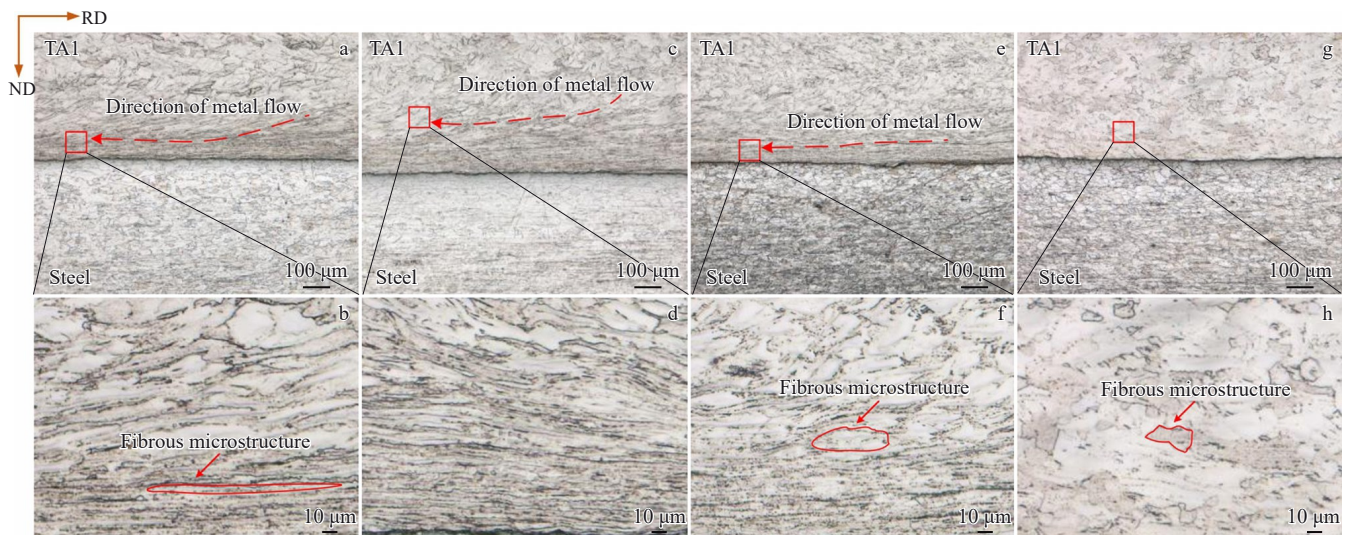


Fig. 5 Cross-section microstructures of TA1/304 composite plates at different states: (a–b) Origin; (c–d) 550 °C; (e–f) 600 °C; (g–h) 650 °C

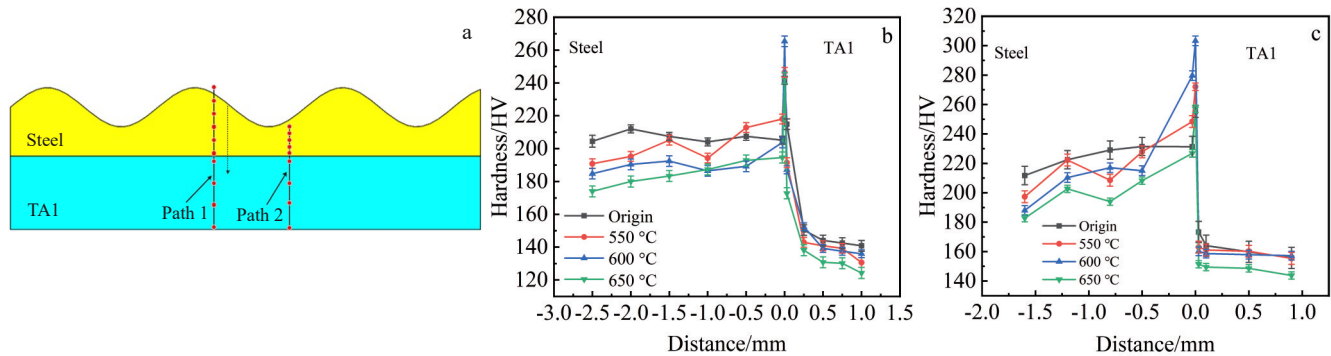


Fig.6 Hardness variations along two paths on the cross-section of specimens after different annealing heat treatments: (a) schematic diagram of hardness measurement points; (b) hardness along Path 1; (c) hardness along Path 2

while annealing alleviates the residual stress and work hardening effect. As the annealing temperature increases, the hardness of the Ti side and the steel side decrease slightly. This is attributed to grain growth in both steel and TA1 sides during the high temperature annealing process.

3.3 Interface element diffusion

EDS line scanning was performed to reveal the diffusion behavior of the elements, as shown in Fig. 7. The results indicate the interface diffusion of the major elements in different interfaces with no obvious diffusion platforms, which suggests the formation of significant solid solution diffusion layers with different thicknesses. The diffusion distance of the elements increases with the increase in annealing temperature. The element diffusion distance of plate without annealing is 2.34 μm . After annealing at 550 and 600 $^{\circ}\text{C}$, the diffusion distance increases to 2.76 and 3.97 μm , respectively. However, it decreases to 2.79 μm when the annealing temperature is 650 $^{\circ}\text{C}$, which may be related to the structural transformation of titanium and the aggregation of elements. It is also worth noting that the elemental diffusion distance of the blue labeled site Fe on the TA1 side in Fig. 7 increases more significantly than that on steel side. This is because the larger atomic gap in Ti makes it easier for Fe to diffuse into Ti. In addition to Fe and Ti, the results of the elemental distributions of Cr and Ni are locally amplified. It is found that the diffusion distance of Cr varies slightly, which is 1.5–2.0 μm . The diffusion distance of Ni in plate after rolling is 1.0 μm , and the diffusion distances of Ni in plate after annealing at 550, 600, and 650 $^{\circ}\text{C}$ are 2.2, 1.5, and 0.8 μm , respectively. The diffusion of Ni to the TA1 side is significant at 550 and 600 $^{\circ}\text{C}$. This suggests that the extent of Ni diffusion during heat treatment may be correlated with the electrochemical corrosion properties of the interface, and further X-ray diffraction (XRD) test of the bonding interface was subsequently conducted.

3.4 Electrochemical testing

The polarization curves of the specimens are shown in Fig. 8. It can be seen that the specimens all show a certain degree of passivation in the corrosion solution. According to the relevant corrosion theory, the lower the corrosion current, the stronger the corrosion resistance of the material surface;

the higher the self-corrosion potential, the stronger the corrosion resistance of the material surface. The self-corrosion potential and self-corrosion current were determined using the Tafel extrapolation method. The results are shown in Table 1 and Table 2. For the rolled surface, the Tafel curves after heat treatment are shifted downward, and the higher the positive value of the corrosion potential, the smaller the tendency to corrosion. It can be seen that the general trend of polarization curves at different temperatures is consistent, and there are obvious passivation regions in plates after annealing at 600 and 650 $^{\circ}\text{C}$. As the heat treatment temperature increases, the current density gradually increases, indicating that the actual corrosion resistance of the TA1 surface is weakened. However, when the heating temperature is 650 $^{\circ}\text{C}$, there is a wide range of stable passivation regions in the corresponding polarization curves. Therefore, the stability of the passivation film on the TA1 surface of the TA1/304 composite plate prepared by this process is weakened by annealing, but the corrosion resistance is stable. Compared with the cladding, corrosion resistance of the cross-section of TA1/304 composite plate is slightly reduced, yet it still exhibits superior corrosion resistance. This is because interfacial bonding and alloying element diffusion occur on both sides of the interface, leading to the precipitation of new Fe-containing phases on the composite plate side. Therefore, the composite plate in the corrosive environment cannot be well protected by the material surface passivation film, resulting in a reduction in corrosion resistance of the composite plate. As can be seen from Fig. 8b, only the specimen annealed at 600 $^{\circ}\text{C}$ exhibits a passivation zone, with the best and most stable corrosion resistance.

The system reached a steady state after the open circuit potential test was completed. AC impedance tests were conducted on the composite plates by applying an AC sinusoidal excitation signal. The Nyquist plots of the TA1/304 composite plates in 3.5wt% NaCl solution are shown in Fig. 9, in which Z parameter is represented by Z. The real part and the imaginary part of the impedance in the results are denoted by Z_{re} and Z_{im} , respectively. It can be seen in Fig. 9a that the higher the annealing temperature, the larger the capacitive arc radius at different heat treatment temperatures. This is because

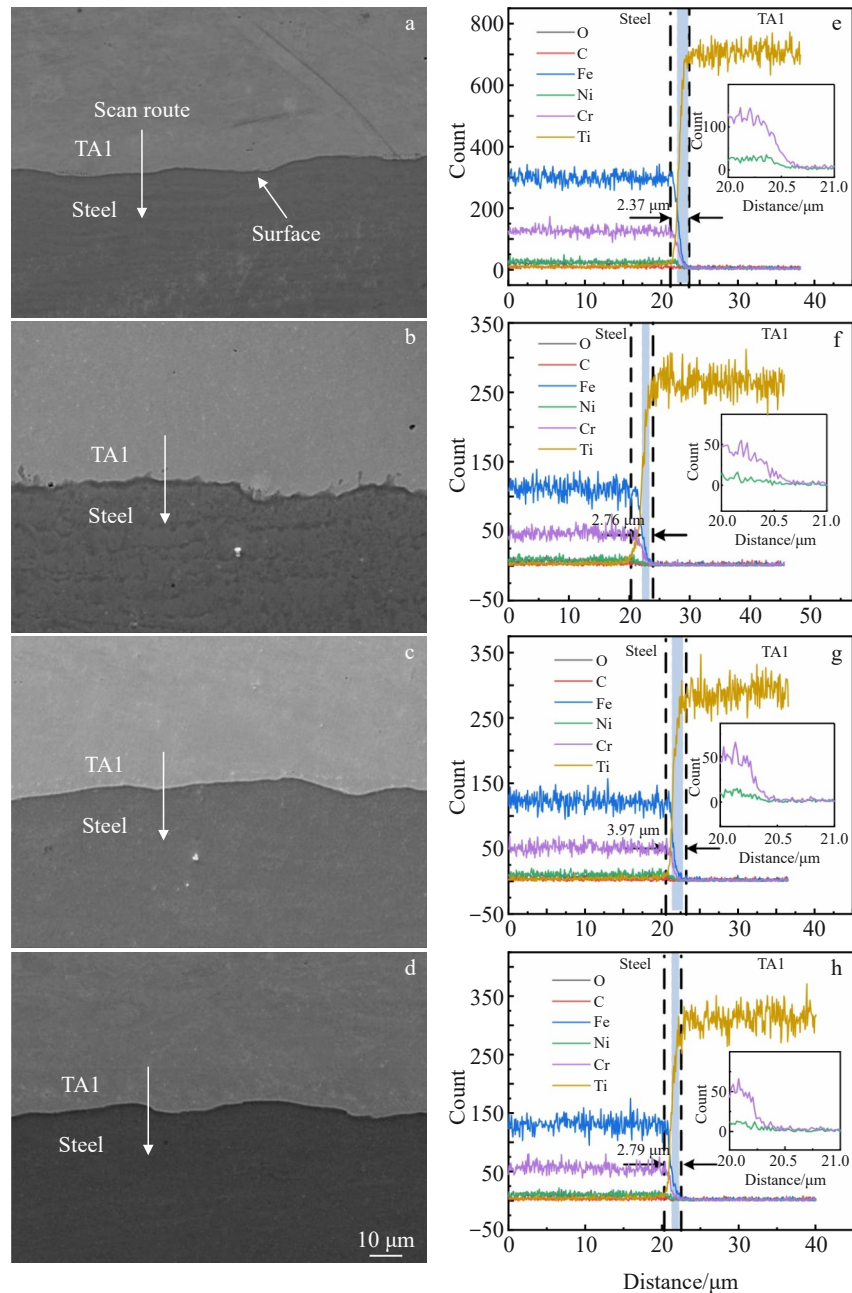


Fig.7 SEM images (a–d) and corresponding EDS line scanning results (e–h) of plates at different states: (a, e) Origin; (b, f) 550 °C; (c, g) 600 °C; (d, h) 650 °C

after annealing at 600 and 650 °C, a passivation zone exists, which can greatly improve the corrosion resistance. However, the rolled specimen exhibits a nearly 45° straight line and a complete impedance arc. This is because there is a dense passivation film on the surface of TA1 at room temperature, which is very stable in nature and can inhibit metal dissolution corrosion. Except for the rolled specimens, all other specimens exhibit a tail consisting of an approximate semicircle and a segment in the low-frequency region. The larger the diameter of the semicircle, the higher the real part of the impedance, indicating better corrosion resistance of the material. As can be seen from Fig.9b, the semicircle radius of the TA1 surface after annealing at 650 °C is large, and the

impedance is large, which coincides with the polarization curve. And there is a dense passivation film on the surface, which is stable in nature. AC impedance curves of cross-section of TA1/304 composite plate in seawater are shown in Fig. 9b. Compared with the radius of the Nyquist plot in Fig.9a, the capacitive arc diameters of the two surfaces differ noticeably. The TA1 surface exhibits a larger capacitive arc diameter, while the cross-section of the TA1/304 composite plate shows a relatively smaller one. This indicates that the passive film formed on the TA1 surface is more stable than that on the cross-section of the TA1/304 composite plate.

In order to more deeply analyze the corrosion resistance of the composite plate, the ZSimpWin software was used to fit

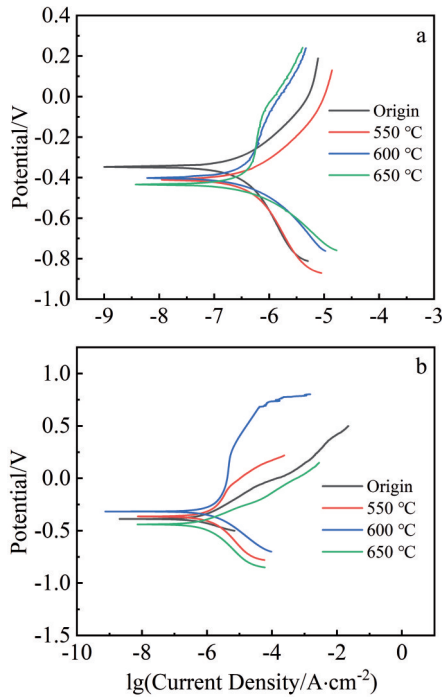


Fig.8 Polarization curves of rolled surface (a) and cross-section (b) of different specimens

the above impedance spectra, and the fitted equivalent circuit is shown in Fig. 9a. R_s is the solution resistance, R_1 is the membrane layer resistance, Q_1 is the membrane layer capacitance, R_2 is the charge transfer resistance, and Q_2 is the double electric layer capacitance. Membrane resistance R_1 usually reflects the ability of corrosive solution to penetrate into the substrate surface. The higher value of R_1 indicates that

Table 1 Polarization curve test results of rolled surface of different specimens

Specimen	Potential/V	Corrosion current, $I/\times 10^{-6}$ A
Origin	-0.346	0.160
550 °C	-0.408	0.229
600 °C	-0.397	0.221
650 °C	-0.431	0.251

Table 2 Polarization curve test results of cross-section of different specimens

Specimen	Potential/V	Corrosion current, $I/\times 10^{-6}$ A
Origin	-0.400	0.715
550 °C	-0.370	0.579
600 °C	-0.320	0.437
650 °C	-0.430	0.871

the membrane layer on the surface of the substrate has a good protection. R_2 usually represents the difficulty of electrochemical reaction. The higher value of R_2 indicates that the charge transfer at the interface and in the solution is more difficult, and the passivation film has a better barrier property. EIS parameters obtained by fitting are shown in Table 3 and Table 4.

The experiments were conducted in 3.5wt% NaCl solution, and a constant potential of 0.5 V was applied to the working electrode through the electrochemical workstation and maintained for 400 s. The data of corresponding current (I) versus time (t) were recorded, and the constant potential polarization curves were plotted, as shown in Fig. 10. The

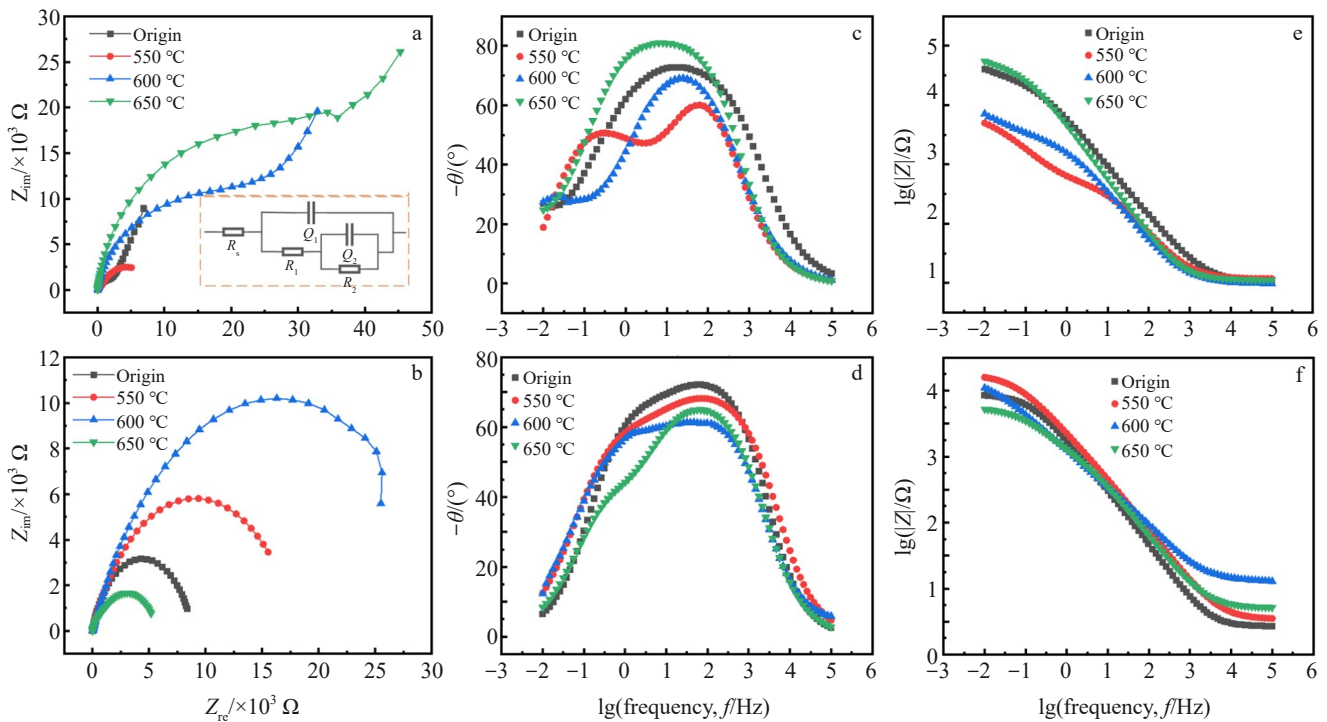


Fig.9 Nyquist plots of TA1/304 composite plates after different heat treatments: (a, c, e) rolled surface; (b, d, f) cross-section

Table 3 EIS parameters of rolled surface of different specimens obtained by fitting

Specimen	$R_s/\Omega \cdot \text{cm}^2$	$R_1/\Omega \cdot \text{cm}^2$	$Y_1/\times 10^{-5} \text{ S} \cdot \text{s}^{n_1} \cdot \text{cm}^{-2}$	n_1	$R_2/\Omega \cdot \text{cm}^2$	$Y_2/\times 10^{-4} \text{ S} \cdot \text{s}^{n_2} \cdot \text{cm}^{-2}$	n_2	χ^2
Origin	10.32	3.104×10^4	3.076	0.8228	2.047×10^4	1.939	0.5642	7.944×10^{-4}
550 °C	11.64	5.514×10^2	8.929	0.7983	7.879×10^3	6.110	0.6995	4.202×10^{-5}
600 °C	9.962	2.936×10^3	8.488	0.7869	1.447×10^5	5.793	0.6317	4.842×10^{-4}
650 °C	11.59	3.362×10^4	3.553	0.9035	1.733×10^5	1.818	0.6474	6.041×10^{-4}

Table 4 EIS parameters of cross-section of different specimens obtained by fitting

Specimen	$R_s/\Omega \cdot \text{cm}^2$	$R_1/\Omega \cdot \text{cm}^2$	$Y_1/\times 10^{-5} \text{ S} \cdot \text{s}^{n_1} \cdot \text{cm}^{-2}$	n_1	$R_2/\times 10^4 \Omega \cdot \text{cm}^2$	$Y_2/\times 10^{-4} \text{ S} \cdot \text{s}^{n_2} \cdot \text{cm}^{-2}$	n_2	$\chi^2/\times 10^{-4}$
Origin	6.657	4.080×10^2	3.490	0.8536	1.913	2.221	0.8000	6.369
550 °C	8.555	5.505×10^3	2.940	0.8017	4.019	2.203	0.6301	2.709
600 °C	14.14	9.598×10^3	3.825	0.8000	8.108	2.736	0.6777	5.897
650 °C	12.71	3.660×10^2	3.923	0.7898	1.055	1.011	0.6884	4.067

curves exhibit the same trend. In the initial stage, with the prolongation of the polarization time, the current increases rapidly, indicating that rapid corrosion occurs on the electrode surface. Subsequently, the current gradually levels off and enters a relatively stable reaction stage, which reflects the difficulty of electrochemical reaction. The results show that the composite plate has different degrees of corrosion tendency after annealing at different temperatures. The specimen annealed at 650 °C exhibits the fastest current increase and reaches the stable stage first, indicating the poorest corrosion resistance. But the current of the specimen annealed at 600 °C increases slowly, indicating the best corrosion resistance. This characteristic has an important effect on metal corrosion resistance. Further analysis reveals that different heat-treated specimens influence the polarization curves via microstructure evolution, which provides a theoretical basis and experimental support for optimizing corrosion resistance.

Fig.11 shows 3D morphologies and cross-section profiles of specimens during corrosion. It can be seen that the height of the TA1 and 304 steel surfaces has distinct characteristics, and that of TA1 reaches 60 μm.

As the microstructure of the material is closely related to its corrosion resistance, and the microstructure of the bonding interface of the rolled composite plate is mainly dependent on its chemical composition and the transient high-temperature and high-pressure effect in the rolling process. Therefore,

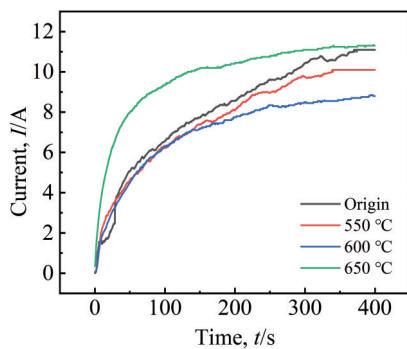


Fig.10 Constant potential polarization curves of different specimens

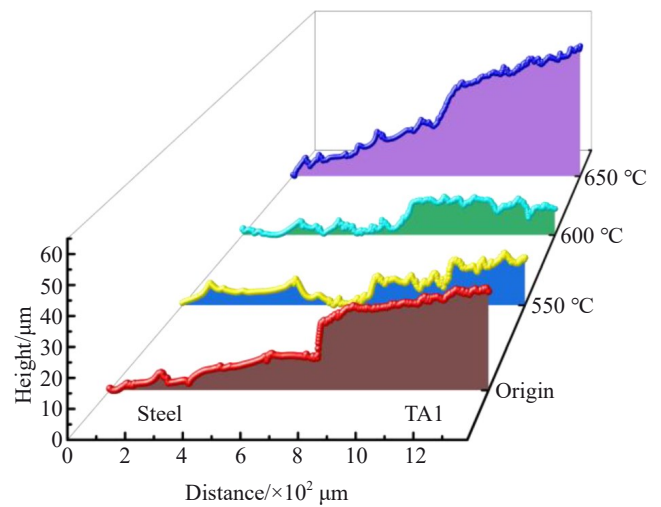


Fig.11 3D morphologies and cross-section profiles of different specimens during corrosion

XRD tests were conducted on the steel side of the bonding interface of the composite plate after annealing at different temperatures. Fig. 12 shows that in addition to the austenite diffraction peak, Ti, Ti₆O, FeNi, and Cr_{0.5}Ni_{0.5} are also detected at the bonding interface of the rolled composite plate without

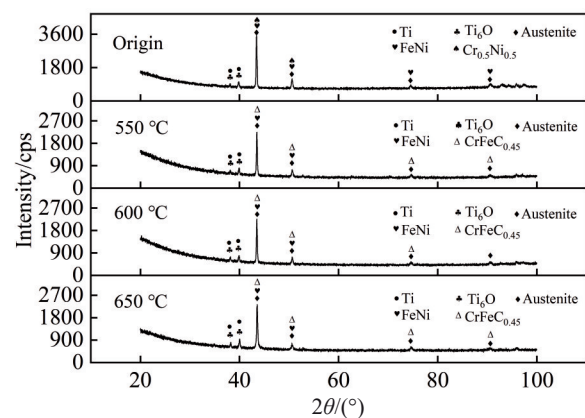


Fig.12 XRD patterns of the steel side of bonding interface of different specimens

heat treatment, while $\text{CrFeC}_{0.45}$ is detected after annealing at different temperatures. Cr-containing compounds are generally brittle and easy to form a passivation film to improve corrosion resistance. Meanwhile, the corrosion resistance of Ni-containing compounds differs as a result of varying Ni content. When the Ni content is low, the compounds are prone to electrochemical corrosion (such as uniform corrosion and pitting). When the Ni content is high, its corrosion resistance will be improved. Due to the insufficient diffusion of element Ni on the steel side of the bonding interface of the rolled composite plate during this process, its Ni content remains relatively high, resulting in corrosion performance inferior to that of the composite plate after heat treatment. And with the change of heat treatment temperature, the generation of $\text{CrFeC}_{0.45}$ may affect the corrosion properties of the composite plate. Of course, corrosion properties are synergistically affected by a number of factors, such as bonding interface compounds and microstructure, and it is not possible to make a representative and accurate analysis of Cr-containing and Ni-containing compounds.

The effect of annealing temperature on the structure and properties of corrugated interface of TA1/304 composite plates is shown in Fig. 13. On the TA1 surface, the corrosion performance is mainly influenced by the microstructure. The variation of hardness is influenced by grain size, and in the passivation environment, the refined grains accelerate the passivation kinetics of the metal. The numerous grain boundaries and triple joints also provide good adhesion to the passivated film layer through the pinning principle, making the passivation film less prone to rupture and dissolution. However, if the grain grown on the TA1 surface is too large, it is not conducive to the formation and extension of the passivation film. Therefore, excessive grain growth on the TA1 surface is not conducive to the formation and extension of the passivation film. Thus, the Origin specimens exhibit the best corrosion resistance on the rolled surface.

In the cross-section, the corrosion behavior is subject to the synergistic effect of bonding interfacial compounds and microstructure. During the annealing treatment of the composite plate, the dislocation density at the bonding interface decreases, defects are reduced, and the microstructure becomes more uniform. This slows down the erosion of the bonding interface

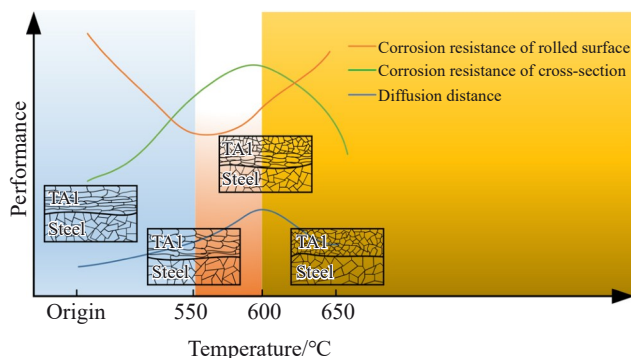


Fig.13 Effect of annealing temperature on properties and microstructure of TA1/304 composite plate

of the composite plate by Cl^- and improves the corrosion resistance of the bonding interface. In a passivation environment, a relatively homogeneous microstructure reduces the density of defects in the passivate film and decreases the geometry of the defects, significantly enhancing the stability of the passivate film and the corrosion resistance. However, different types of Cr-containing and Ni-containing compounds are generated at the bonding interface, and the presence of these compounds may have a very unfavorable effect on the corrosion resistance of the material. So, the rolled surface of specimens annealed at $600\text{ }^\circ\text{C}$ has the best corrosion resistance.

4 Conclusions

1) After heat treatment, the grain distribution at TA1 side of the composite plate is uniform, and the fibrous microstructure at steel side gradually becomes equiaxed, thus enabling the element distribution and corrosion properties of the composite plate to change regularly.

2) Heat treatment promotes the diffusion of elements at the interface of TA1/304 composite plate, which results in the formation of different combinations at the interface. At $600\text{ }^\circ\text{C}$, the diffusion distance of interface elements reaches $3.97\text{ }\mu\text{m}$.

3) The electrochemical corrosion test results show that the rolled surface and cross-section of the composite plate will show passivation characteristics in artificial seawater, but only for the plates treated at specific heat treatment temperature. The self-corrosion current on the surface of TA1 is low, and the surface passivation film is more complete. When the heat treatment temperature is below $650\text{ }^\circ\text{C}$, the lower the heat treatment temperature, the smaller the radius of capacitive arc, and the higher the current density. And at the cross-section of composite plate, when the heat treatment temperature is below $600\text{ }^\circ\text{C}$, the higher the heating temperature, the larger the capacitive arc radius and the lower the current density. And the corrosion resistance of rolled surface is better than that of the cross-section. So, the rolled surface of specimen annealed at $600\text{ }^\circ\text{C}$ exhibits best corrosion resistance, which fully meets the corrosion resistance requirements of the composite plate in practical applications.

4) The interface microstructure analysis shows that the diffusion of alloying elements at the bonding interface of the TA1/304 composite plate and the formation of $\text{CrFeC}_{0.45}$ in the bonding area near the TA1 side are the main reasons for the decrease in corrosion resistance of the TA1/304 composite plate.

References

- 1 Jing J Q, Guo J, Li B et al. *Journal of Iron and Steel Research International*[J], 2021, 28(8): 1
- 2 Xin Q Y, Bin Z Z, Kun Y H et al. *Journal of Iron and Steel Research International*[J], 2023, 30(8): 1463
- 3 Zhou Q, Su C Y, Zheng J J. *Surface & Coatings Technology*[J],

- 2020, 389: 125649
- 4 Zhou X F, Lv X Y, Wu S J et al. *Journal of Materials Engineering and Performance*[J], 2025, 34(6): 5063
- 5 Luo L, Duan X M, Ma W J et al. *Rare Metal Materials and Engineering*[J], 2022, 51(7): 2420
- 6 Yang X Y, Guo K, Gao Y Z et al. *Materials Science & Engineering A*[J], 2021, 824: 141802
- 7 Pan Y Z, Zuo H B, Wang J S et al. *Journal of Iron and Steel Research International*[J], 2019, 26(10): 1126
- 8 Zhou Q, Jia B, Guo B Q et al. *International Journal of Mechanical Sciences*[J], 2022, 225: 107362
- 9 Zhou B B, Ye C, Zhang B J et al. *Rare Metal Materials and Engineering*[J], 2020, 49(1): 59
- 10 Wang Y, Wang T, Ren Z K et al. *Journal of Materials Processing Technology*[J], 2022, 310: 117782
- 11 Duan J Z, Liu H, Dong P C et al. *Materials and Corrosion*[J], 2022, 73(6): 887
- 12 Garbacz H, Pisarek M, Kurzydłowski K J. *Biomolecular Engineering*[J], 2007, 24(5): 559
- 13 Hoseini M, Shahryari A, Omanovic S et al. *Corrosion Science*[J], 2009, 51(12): 3064
- 14 Cvijović -Alagić I, Cvijović Z, Bajat J et al. *Corrosion Science*[J], 2014, 83: 245
- 15 Mudali U K, Rao B M A, Shanmugam K et al. *Journal of Nuclear Materials*[J], 2003, 321(1): 40
- 16 Liu Y C, Zheng Z B, Xu L L et al. *Corrosion Science*[J], 2024, 230: 111923
- 17 Lu L Y, Su Y, Chen J et al. *Materials Research Express*[J], 2020, 7(2): 025012
- 18 Li N N, Wang B Q, Liu T et al. *Corrosion Science*[J], 2024, 233: 112107
- 19 Pu J, Chen T, Sun Y et al. *Coatings*[J], 2024, 14(9): 1175
- 20 Tan H B, Zhao Z B, Yang J X et al. *Rare Metal Materials and Engineering*[J], 2022, 51(12): 4385

热处理温度对TA1/304复合板微观组织和耐腐蚀性能的影响

李熙杰¹, 李志鹏¹, 刘江林^{1,2,3}, 赵林超¹, 唐宇平¹, 梁建国^{1,2,3,4}

(1. 太原理工大学 机械工程学院, 山西 太原 030024)

(2. 先进金属复合材料成形技术与装备教育部工程研究中心, 山西 太原 030024)

(3. 金属成形技术与重型装备全国重点实验室, 山西 太原 030024)

(4. 新疆智能装备研究院, 新疆 阿克苏 843000)

摘要: 通过模拟TA1/304复合板在人工海水(3.5wt% NaCl溶液)中的电化学实验,研究了该复合板经不同温度热处理后的耐腐蚀性能和腐蚀机理,分析了界面扩散行为和微观结构演变。结果表明,界面元素的扩散范围和扩散层的厚度随加热温度的不同而变化。由于其特殊的结构和成分,TA1/304复合板在含Cl⁻的腐蚀介质中表现出优异的耐腐蚀性能,且其耐腐蚀性能明显优于普通钢板。同时,研究发现复合板的热处理工艺对其耐腐蚀性能有显著影响,经过600℃退火热处理后,复合板的耐腐蚀性能得到提高,且轧制表面的耐腐蚀性能远优于横截面。该研究成果为TA1/304复合板在化工、海洋工程等对耐腐蚀性能要求严格的领域的进一步应用提供了重要的理论依据和技术支撑。

关键词: 钛/钢复合板; 热处理温度; 金相组织; 电化学腐蚀; 扩散行为

作者简介: 李熙杰,男,2000年生,硕士,太原理工大学机械工程学院,山西太原030024, E-mail: 2528626443@qq.com